WISC

UNIVERSITY OF WISCONSIN • MADISON, WISCONSIN

PLASMA PHYSICS

REDUCING AND MEASURING FLUCTUATIONS IN THE MST RFP: ENHANCEMENT OF ENERGY CONFINEMENT and MEASUREMENT OF THE MHD DYNAMO

D. J. DEN HARTOG,[1] A. F. ALMAGRI,[1] M. CEKIC,[2] B. E. CHAPMAN,[1] J. T. CHAPMAN,[1] C.-S. CHIANG,[1] D. CRAIG,[1] N. C. CROCKER,[1] G. FIKSEL,[1] P. W. FONTANA,[1] A. K. HANSEN,[1] C. C. HEGNA,[1] H. JI,[3] N. E. LANIER,[1] K. A. MIRUS,[1] S. C. PRAGER,[1] J. S. SARFF,[1] J. C. SPROTT,[1] M. R. STONEKING,[1] and E. UCHIMOTO[4]

DOE/ER/54345-281 September 1996

UNIVERSITY OF WISCONSIN MADISON

ONSIN

nvited talk t en e Sixt u rgy Co
Mo réal, Cana C 996.

NOTICE

Printed in the United States of America
Available from
National Technical Information Service
U.S. Department of Commerce
5285 Port Royal Road
Springfield, VA 22161

NTIS Price codes
Printed copy: A02
Microfiche copy: A01

Abstract

REDUCING AND MEASURING FLUCTUATIONS IN THE MST RFP: ENHANCEMENT OF ENERGY CONFINEMENT and MEASUREMENT OF THE MHD DYNAMO.

A three- to five-fold enhancement of the energy confinement time in a reversed-field pinch (RFP) has been achieved in the Madison Symmetric Torus (MST) by reducing the amplitude of tearing mode fluctuations responsible for anomalous transport in the core of the RFP. By applying a transient poloidal inductive electric field to flatten the current density profile, the fluctuation amplitude $\tilde{b}/B$ decreases from 1.5% to 0.8%, the electron temperature T_{e0} increases from 250 eV to 370 eV, the ohmic input power decreases from 4.5 MW to approximately 1.5 MW, the poloidal beta β_θ increases from 6% to 9%, and the energy confinement time τ_E increases from 1 ms to ~5 ms in I_ϕ = 340 kA plasmas with density $\bar{n} = 1\times10^{19}\,\mathrm{m}^{-3}$. Current profile control methods are being developed for the RFP in a program to eliminate transport associated with these current-gradient-driven fluctuations. In addition to controlling the amplitude of the tearing modes, we are vigorously pursuing an understanding of the physics of these fluctuations. In particular, plasma flow, both equilibrium and fluctuating, plays a critical role in a diversity of physical phenomena in MST. The key results: 1) Edge probe measurements show that the MHD dynamo is active in low collisionality plasmas, while at high collisionality a new mechanism, the "electron diamagnetic dynamo," is observed. 2) Core spectroscopic measurements show that the toroidal velocity fluctuations of the plasma are coherent with the large-scale magnetic tearing modes; the scalar product of these two fluctuating quantities is similar to that expected for the MHD dynamo electromotive force. 3) Toroidal plasma flow in MST exhibits large radial shear and can be actively controlled, including unlocking locked discharges, by modifying E_r with a robust biased probe.

1. INTRODUCTION

A three- to five-fold enhancement of the energy confinement time in a reversed-field pinch (RFP) has been achieved in the Madison Symmetric Torus (MST) by reducing the amplitude of tearing mode fluctuations responsible for anomalous transport in the core of the RFP. By applying a transient poloidal inductive electric field to flatten the current density profile, the fluctuation amplitude $\tilde{b}/B$ halves, the electron temperature T_{e0} increases, the ohmic input power decreases, the poloidal beta β_θ increases from 6% to 9%, and the energy confinement time τ_E increases from 1 ms to ~5 ms in I_ϕ = 340 kA plasmas. The ion temperature is unchanged, so the ion to electron temperature ratio decreases as might be expected from reduced anomalous ion heating associated with reduced fluctuations. Additionally the radiated power, including bremsstrahlung and H_α, are reduced ~50%, indicating that the plasma is cleaner and that the global particle confinement time is substantially increased. At I_ϕ = 440 kA, a record high (for MST) electron temperature T_{e0} = 600 eV is obtained, although at somewhat lower beta ($\beta_\theta \approx 7.5\%$) but with similar energy confinement ($\tau_E \sim 5$ ms). A robust feature of inductive poloidal current drive is the elimination of sawtooth oscillations. In our first inductive poloidal current drive experiments

[1], the magnetic fluctuation amplitude was maintained at the low "between-sawtooth-crash" value when inductive poloidal current drive was present. With improved current drive (longer duration and more uniform amplitude), the fluctuation amplitude in many discharges falls below the between-sawtooth-crash value, and the parameters listed above are achieved. An intriguing and encouraging aspect of these experiments is that only modest inductive poloidal current drive (about 25% of the total poloidal current) was required to produce low fluctuation amplitudes.

In addition to controlling the amplitude of the tearing modes as described above, we are vigorously pursuing an understanding of the physics of these fluctuations. In particular, a series of experiments has been carried out in the the RFP to measure the dynamo electric field parallel to the equilibrium magnetic field. This dynamo arises from the correlation between the fluctuating flow velocity and magnetic field. In the edge plasma, the fluctuating flow velocity is obtained from probe measurement of the fluctuating $\mathbf{E}\times\mathbf{B}$ drift and the electron diamagnetic drift [2]. In low collisionality edge plasmas the pressureless MHD dynamo appears to be active (the fluctuating velocity is dominated by the $\mathbf{E}\times\mathbf{B}$ drift), while at high collisionality, a new "electron diamagnetic dynamo" is observed (the fluctuating velocity is dominated by the diamagnetic drift) [3]. Since probe techniques cannot access the core plasma or measure the plasma velocity directly, we are employing spectroscopic Doppler measurements of impurity ions to achieve these goals. The toroidal velocity fluctuations in the core plasma and the core tearing mode magnetic fluctuations exhibit coherence below ~15 KHz, indicating that both these quantities are large-scale MHD fluctuations of the order of the plasma size. The velocity fluctuation amplitude and the magnetic fluctuation amplitude grow in magnitude and peak at the sawtooth crash. The scalar product of $|\tilde{v}_\phi|$ and $|\tilde{b}_r|$ exhibits the sawtooth cycle time variation expected for the dynamo electromotive force in MST. In addition to the dynamo, plasma flow also plays a critical role in a diversity of physical phenomena in MST, e.g., magnetic mode rotation and locking, and radial electric field profiles.

2. POLOIDAL INDUCTIVE CURRENT DRIVE FOR FLUCTUATION REDUCTION

In conventional RFP operation, an inductive electric field applied toroidally drives the plasma current. In this experiment, we also apply an inductive poloidal electric field. When this field is applied, the electric field parallel-to-B is increased most in the outer region of the plasma (where the magnetic field is largely poloidal). This facilitates current profile flattening for fluctuation suppression. Inductive poloidal current drive is inherently transient since it produces a changing toroidal flux Φ_ϕ in the plasma volume. The observed improvements last as long as poloidal current drive is present. To distinguish poloidal inductive current drive from conventional RFP operation and as a reminder of the transient nature of this current drive technique, we refer to this experiment as pulsed poloidal current drive (PPCD). With PPCD, the magnetic fluctuation amplitude drops to roughly half its normal value, the electron temperature increases to a record high (for MST) of ~600 eV, and the plasma resistance dramatically decreases. As a result of the decreased plasma

resistance and increased stored thermal energy, the global energy confinement time is dramatically increased.

The waveforms of the poloidal and toroidal components of the electric field E_θ and E_ϕ (measured at the plasma surface), the current I_ϕ, the average toroidal magnetic field $\langle B_\phi \rangle = \Phi_\phi / \pi a^2$, and the toroidal field at the surface $B_\phi(a)$ during a PPCD experiment are shown in Fig. 1. The shaded region indicates the time during which the PPCD programming is applied. In the first PPCD experiment [1], the E_θ drive was a single, triangular shaped pulse. Figure 1 illustrates the recently improved PPCD programming that provides a series of four smaller pulses. The improved system drives poloidal current more uniformly throughout the PPCD phase and reduces the plasma-wall interaction, since the E_θ amplitude does not need to be as large. Also, PPCD lasts longer, maintaining the beneficial effects observed in the first experiment for a longer period of time. The sharp negative spikes in E_θ both before and after PPCD are associated with plasma-generated toroidal flux from spontaneous sawtooth (discrete dynamo) events (see Fig. 1c). The E_θ spikes during these events are a result of the passage of toroidal flux through the poloidal break in the conducting shell surrounding the plasma. In contrast, PPCD is a controlled increase in the poloidal current through application of positive E_θ.

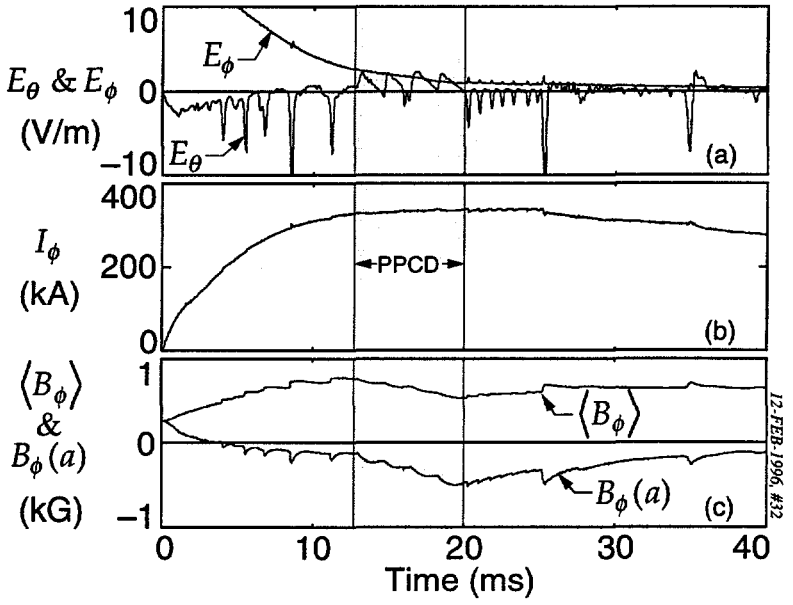

Fig. 1. Waveforms of (a) the surface electric field components, inferred from loop voltages, (b) the toroidal plasma current, and (c) the toroidal magnetic field during PPCD.

A key result of improved PPCD is a greater reduction of the magnetic fluctuation amplitude, resulting in more dramatic improvements in energy confinement and other measures of plasma quality. The spatial rms magnetic field fluctuation measured in an improved PPCD discharge by a toroidal array of 32 pickup coils on the plasma surface is shown in Fig. 2a, normalized to the equilibrium field strength. (The dominant wavelengths that compose this fluctuation are m = 1, n = 6-10 modes.) Before PPCD is applied, the fluctuation

amplitude cycles with the sawtooth oscillation. PPCD suppresses sawtoothing, and the fluctuation amplitude first grows slowly and then decreases. Sawteeth are suppressed in virtually all PPCD discharges, but the fluctuation amplitude most often holds at the "between sawtooth crash" value. With improved PPCD programming, the fluctuation amplitude in some discharges (like that of Fig. 2) is reduced below the sawtooth cycle minimum value to record low values. During these periods of very low fluctuation, the improvements in the plasma are most dramatic. The parallel electric field $E_\parallel = \mathbf{E} \cdot \mathbf{B} / B$ measured at the plasma surface is shown in Fig. 2b to emphasize the relationship of reduced magnetic fluctuation and poloidal current drive. While poloidal current is driven by PPCD, the fluctuation amplitude is small.

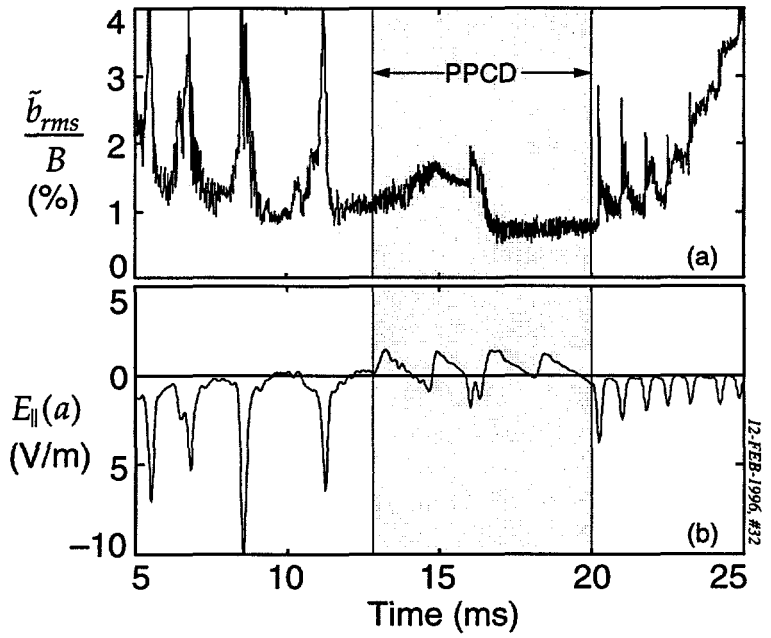

Fig. 2. The (a) spatial rms magnetic fluctuation and (b) the parallel electric field measured at the plasma surface during a PPCD discharge formed with improved poloidal current drive.

In a conventional RFP, the tearing fluctuations generate large overlapping magnetic islands that destroy closed magnetic surfaces. The measured fluctuation-induced heat and particle fluxes in MST are large in the plasma core (inside the reversal surface) where the tearing modes resonate [4,5]. During inductive current profile control, the fluctuation amplitudes are reduced and fall near or below estimated island overlap thresholds. It is possible that closed magnetic surfaces form, although the residual fluctuations still produce closely-spaced islands of width $w/a \sim 0.05$ (about 80% of that required for island overlap).

The global energy confinement time τ_E increases during PPCD as a result of both increased stored thermal energy and decreased plasma resistance, i.e., decreased ohmic input power P_{ohmic}. The shot-averaged line density $\bar{n}_e$, central electron pressure $n_{e0} kT_{e0} P_{ohmic}$, mean-squared magnetic fluctuation $\tilde{b}^2$, and H_α

radiation for 100 PPCD plasmas are shown in Fig. 3. The same quantities from 80 conventional RFP plasmas are overlayed for comparison. The central electron pressure is measured with a single point (time and space) Thomson scattering diagnostic, varied in time shot-by-shot. In estimating τ_E and β_θ, the $nk(T_e + T_i)$ radial profile is assumed to behave as $[1 - (r/a)^2]$. (An 11-chord interferometer indicates the density profile is centrally peaked, but the temperature profiles are not measured.) The ion temperature measured by charge exchange is $T_i^{cx} \approx 0.5 T_{e0}$ in conventional discharges at this density but remains constant while T_{e0} increases by as much as 170% during PPCD. The ohmic input power is derived from the measured total input power (Poynting flux) at the plasma surface by subtracting the rate of change of stored magnetic energy using equilibrium modeling. (The calculation includes power from both E_θ and E_ϕ.) Most of the PPCD plasmas in this ensemble are "ordinary" in that τ_E increases during PPCD from 1.2 ms to ~4 ms and β_θ increases from 6% to ~8%. A subset ensemble of 25 superior PPCD plasmas which exhibit the exceptionally low magnetic fluctuation level features illustrated in Fig. 2a have confinement times $\tau_E \sim 5$ ms and $\beta_\theta \sim 9\%$. Table I summarizes the best PPCD confinement in comparison with conventional RFP confinement at medium current of 340 kA. An MST record $T_{e0} = 615$ eV was measured for similar superior discharges at 440 kA and $\bar{n}_e \approx 1 \times 10^{19}$ m^{-3}, at somewhat lower beta $\beta_\theta \sim 7.5\%$ but similar $\tau_E \sim 5$ ms.

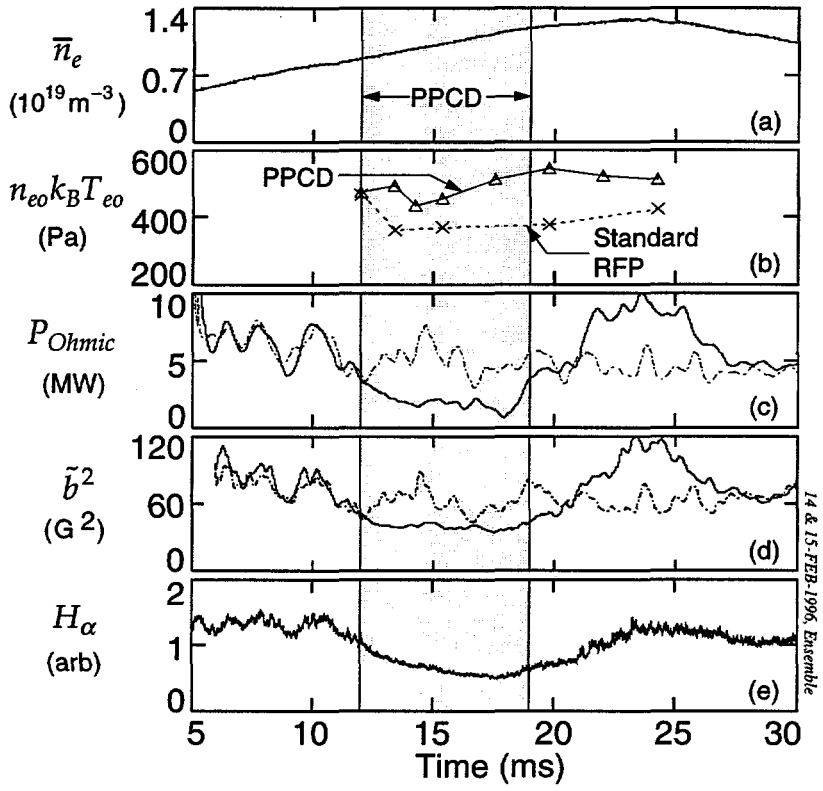

Fig. 3. Shot-averaged waveforms of (a) the central chord line average density, (b) central electron pressure from Thomson scattering, (c) ohmic input power, (d) mean-squared fluctuation amplitude, and (e) H_α radiation. The unbroken lines are for 100 PPCD discharges, and the broken lines are for 80 standard RFP discharges.

TABLE I. MST CONFINEMENT PARAMETERS WITH AND WITHOUT PPCD

	PPCD	**Conventional RFP**
Current, I_ϕ	340 kA	340 kA
Density, n_e	1.0×10^{19} m^{-3}	1.0×10^{19} m^{-3}
Temperature, T_{e0}	390 eV	230 eV
Beta, β_θ	9%	6%
Input power, P_Ω	1.45 MW	4.4 MW
Confinement, τ_E	4.8 ms	1.1 ms

PPCD clearly demonstrates a connection between current profile control, fluctuation suppression, and reduced transport, but it is inherently transient and greater improvement is desirable. Electrostatic and rf current drive can in principle enhance and sustain current profile control. An electrostatic current injection experiment using plasma-based current sources [6] placed at the edge of the plasma is in progress. The system will provide up to 15 kA of current from 15 localized sources, enough to test tearing stablilization in lower current MST plasmas according to MHD theoretical computation [7]. In the longer term, rf current drive could be the ideal solution, easily targeted to specified locations in the plasma. The lower-hybrid wave has been identified a good candidate for efficient edge poloidal current drive in typical MST plasmas. Initial accessibility and ray tracing calculations [8] are currently being refined.

3. EQUILIBRIUM AND FLUCTUATING PLASMA FLOW

3.1 Edge probe measurements of the dynamo

Spontaneous self-generation of magnetic field in a plasma, the "dynamo effect," is a ubiquitous phenomenon in astrophysical plasmas and occurs in laboratory plasmas such as the RFP and spheromak. In the RFP, the magnetic field, or plasma current parallel to the field, cannot be fully accounted for by the applied toroidal electric field. This is dramatically evident in the outer region of the plasma where the applied parallel electric field is either zero or actually points in the direction opposite to the observed current.

Theoretical study of the RFP dynamo has progressed quite far. The most thoroughly studied mechanism is the MHD dynamo, in which the current is self-generated by the $\langle \tilde{\mathbf{v}}\times\tilde{\mathbf{B}}\rangle$ term in Ohm's law, where $\langle\ \rangle$ denotes an average over a magnetic surface. However, there is a second dynamo term in the parallel Ohm's law that appears to be important [9, 10]:

$$\eta_\parallel j_{\parallel 0} - E_{\parallel 0} = \langle \tilde{\mathbf{v}}\times\tilde{\mathbf{B}}\rangle_\parallel - \langle \tilde{\mathbf{j}}\times\tilde{\mathbf{B}}\rangle_\parallel / en \tag{1}$$

$$= \langle \tilde{\mathbf{E}}_\perp \cdot \tilde{\mathbf{b}}_\perp \rangle + \langle \nabla_\perp \tilde{P}_e \cdot \tilde{\mathbf{b}}_\perp \rangle / en \tag{2}$$

where $\mathbf{b}\equiv\mathbf{B}/B$. The first term on the right-hand-side of Eq. (2), $\langle \tilde{\mathbf{E}}\cdot\tilde{\mathbf{b}}_\perp\rangle$, represents the contribution to $\tilde{\mathbf{v}}_{e\perp}$ from the fluctuating $\tilde{\mathbf{E}}_\perp\times\mathbf{B}_0$ drift, which is a

MHD (single fluid) effect. This term, then, represents the MHD dynamo. The second term, $\langle \nabla \tilde{P}_e \cdot \tilde{\mathbf{b}} \rangle / en$, is the contribution from the fluctuating electron diamagnetic drift $\nabla \tilde{P}_e \times \mathbf{B}_0$ which is an electron fluid effect (in a two-fluid framework).

In MST, collisionality (as measured by the ratio of the electron mean free path λ_e to the minor radius a) is low, on the order of 2-7. The MHD dynamo dominates in MST plasmas where the coherence at the dominant tearing mode frequencies of the $\langle \tilde{\mathbf{E}} \cdot \tilde{\mathbf{b}} \rangle$ term is much greater than that of the $\langle \nabla \tilde{P}_e \cdot \tilde{\mathbf{b}} \rangle / en$ term. The dynamo term also dominates in low density, low collisionality TPE-1RM20 plasmas. However, in high density TPE-1RM20 plasmas, $\lambda_e/a < 1$, the coherence exhibited by the diamagmetic term $\langle \nabla \tilde{P}_e \cdot \tilde{\mathbf{b}} \rangle / en$ dominates that of the $\langle \tilde{\mathbf{E}} \cdot \tilde{\mathbf{b}} \rangle$ term. In this case, the diamagnetic term is large enough to drive the parallel current required by the dynamo in the edge of the RFP. The physical reason for the transition by collisions from MHD to diamagnetic dynamo is not clear. However, it is interesting to note that the diamagnetic dynamo term can be rewritten as $\langle \nabla \tilde{P}_e \cdot \tilde{\mathbf{b}} \rangle \approx \nabla \cdot \langle \tilde{P}_e \tilde{\mathbf{b}} \rangle$, where the quantity $\langle \tilde{P}_e \tilde{\mathbf{b}} \rangle$ can be regarded as electron momentum (current) flux transported by magnetic fluctuations. This is the idea behind the kinetic dynamo effect [11], although this measurement cannot distinguish whether it is present.

3.2 Spectroscopic measurements of velocity fluctuations

Since the plasma flow velocity $\mathbf{v}=(m_i\mathbf{v}_i+m_e\mathbf{v}_e)/(m_i+m_e) \approx \mathbf{v}_i$, spatially localized measurement of $\tilde{\mathbf{v}}_i$ and its correlation with $\tilde{\mathbf{B}}$ is the most direct way to measure the MHD dynamo term $\langle \tilde{\mathbf{v}} \times \tilde{\mathbf{B}} \rangle$. Our measurement technique on MST [12] approximates the ideal of local measurements of the majority species dynamics in two ways. First, our diagnostic records impurity ion dynamics, specifically the Doppler shift and broadening of naturally occuring impurity ion line emission. However, on the time and spatial scales of interest, the impurities should mimic majority species behavior. The second and more problematic approximation to the ideal measurement arises from the fact that our diagnostic passively records a chord-average of the impurity ion emission. Analysis of such data for spatial correlation measurements requires detailed knowledge of the impurity emission profiles in conjunction with careful modeling of the structure of the dominant tearing modes. In spite of these difficulties we have begun to assemble a direct, quantitative measurement of MHD dynamo activity in an RFP.

Dynamo activity in MST is manifested in two distinct ways, a discrete and a continuous dynamo. The discrete dynamo is evident during a sawtooth event [13]. Sawtooth events occur in MST with a period of about 3 ms. Figure 4 illustrates the field generation and relaxation that occurs over a sawtooth oscillation. Strong spontataneous magnetic field generation is evident in the sudden increase of toroidal flux Φ_ϕ during a sawtooth crash (at $t = 0$ in Fig. 4). The peak of the time derivative of the toroidal flux, measurable as the surface poloidal electric field E_θ, is employed as a time reference for the sawtooth crash. The decreases in the pinch parameter $\Theta \equiv B_\theta(a)/(\Phi_\phi/\pi a^2)$ and the reversal parameter $F \equiv B_\phi(a)/(\Phi_\phi/\pi a^2)$ indicate that, during a crash, the plasma relaxes toward a minimum energy state with a flatter current profile, i.e., current decreases at the core and increases at the edge. Between crashes, flux generation (opposing resistive decay) is present at a low level, indicating operation of a continuous dynamo.

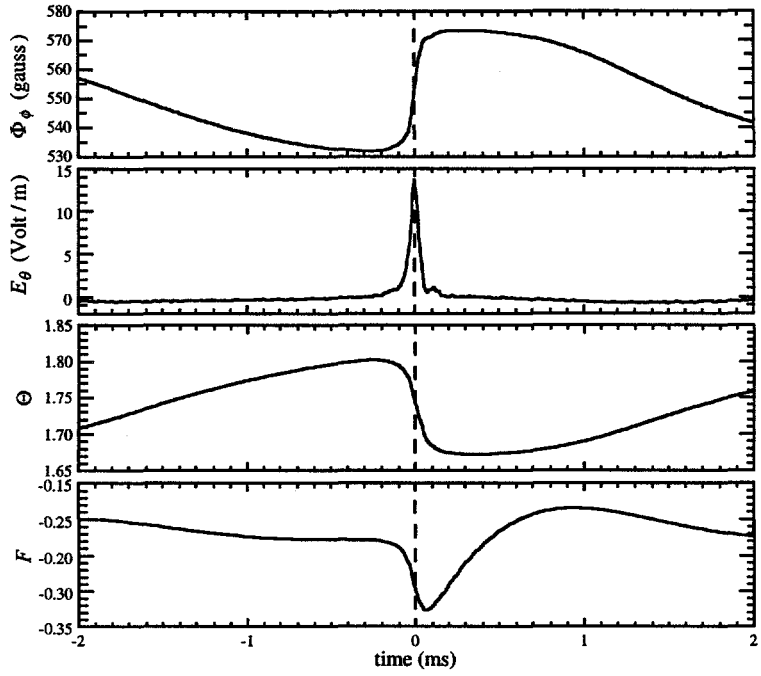

Fig. 4. An ensemble average over 442 sawtooth events illustrating the sawtooth oscillation in toroidal flux Φ_ϕ, surface poloidal electric field E_θ, pinch parameter Θ, and reversal parameter F.

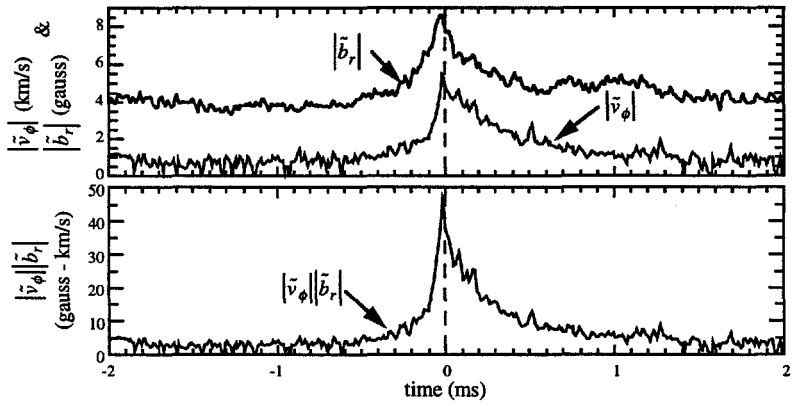

Fig. 5. Sawtooth ensemble-average of $|\tilde{v}_\phi|$ and $|\tilde{b}_r|$, and the scalar quantity $|\tilde{v}_\phi||\tilde{b}_r|$.

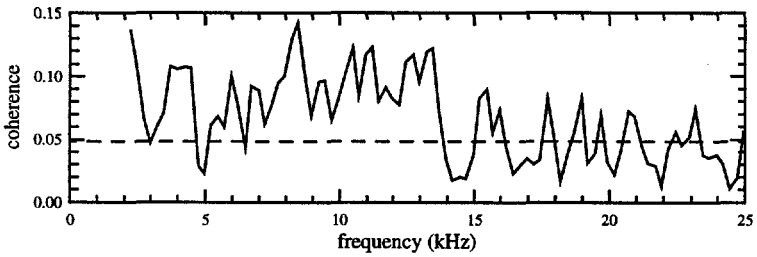

Fig. 6. Coherence amplitude of $\tilde{v}_\phi$ and $\tilde{b}_r$, the dashed line indicates the noise level.

Figure 5 illustrates our ensemble-averaged (equivalent to an average over a flux surface) measurement of the MHD dynamo quantities $|\tilde{v}_\phi|$ and $|\tilde{b}_r|$. Note how both the velocity fluctuation amplitude and the magnetic fluctuation amplitude grow in magnitude and peak at the sawtooth crash. These quantities are coherent between 5 - 15 kHz (Fig. 6), indicating that they are representative of the long-wavelength tearing modes expected to be associated with the MHD dynamo in the RFP [14]. The scalar quantity $|\tilde{v}_\phi||\tilde{b}_r|$ is also shown in Fig. 5. As expected, this quantity is non-zero throughout the sawtooth cycle (indicating the operation of a continuous dynamo) and peaks during the sawtooth crash (indicative of the discrete dynamo). Calculation of the cross product of $\tilde{v}_\phi$ and $\tilde{b}_r$, which is the actual MHD dynamo term, is in process. Determination of the phase between $\tilde{v}_\phi$ and $\tilde{b}_r$ is complicated by the fact that the measured $\tilde{v}_\phi$ is chord-averaged, but initial analysis indicates that the correlation phase provides for a substantial non-zero dynamo electromotive force.

3.3 Equilibrium plasma flow, magnetic mode rotation, and E_r

Plasma flow, magnetic mode rotation, and radial electric field are tightly coupled in MST. The dominant tearing mode fluctuations (which are core resonant) generally phase lock together and co-rotate [15]. The toroidal flow of the core impurity C V ions closely tracks the toroidal phase velocity of the dominant tearing modes. This tracking is especially striking during a sawtooth event when fast changes in toroidal rotation occur [16]. The deceleration time of the magnetic modes and the plasma is about 100 μs, with the modes leading the plasma by about 10 μs. The deceleration of the modes is as expected from a calculation of the electromagnetic torque on a magnetic island, but a simple calculation of the Braginskii viscous diffusion of the plasma predicts a much longer deceleration time for the toroidal flow velocity. However, this discrepancy can be resolved by accounting for the presence of a number of phase-locked $m = 1$ islands in a diffusive toroidal momentum transport model calculation [17]. The nonlinear interaction of these tearing modes also appears to play a prominant role in momentum degradation and mode locking [18].

Impurity ion states midway between the core and edge (B IV and O V) and in the edge (C III) provide a rough picture of the flow profile; the toroidal plasma flow appears to slow down and even reverse direction near the edge. The oppositely directed flow of the edge plasma may be due to the fact that the radial electric field E_r changes sign at the reversal surface, pointing radially *out* inside the surface and radially *in* outside the surface [19]. E_r can be dramatically altered by the insertion of a biased probe into the plasma; this technique provides control of the rotation of the plasma, including unlocking and spinup of locked discharges [20].

4. SUMMARY

The fluctuation amplitude of the dominant magnetic tearing modes in MST has been halved by application of a transient poloidal inductive electric field to flatten the current density profile. This resulted in an approximate quadrupling of the energy confinement time τ_E to 5 ms and an increase in poloidal beta β_θ from 6% to 9%. The magnetic fluctuations in MST are coherent

with fluctuations in the plasma toroidal flow velocity, indicative of MHD dynamo current generation. In higher collisionality RFP plasmas, a new mechanism, the "electron diamagnetic dynamo," is observed.

ACKNOWLEDGEMENT

This work was supported by the U. S. Department of Energy.

REFERENCES

[1] J. S. SARFF, S. A. HOKIN, H. JI, S. C. PRAGER, and C. R. SOVINEC, Phys Rev. Lett. **72** (1994) 3670; J. S. SARFF *et al.*, Phys. Plasmas **2** (1995) 2440.

[2] H. JI, A. F. ALMAGRI, S. C. PRAGER and J. S. SARFF, Phys. Rev. Lett. **73** (1994) 668; H. JI *et al.*, Phys Rev Lett **74** (1995) 1086.

[3] Work done in collaboration with the TPE-1RM20 group (Y. YAGI, K. HATTORI, Y. HIRANO, T. SHIMADA, Y. MAEJIMA, and K. HAYASE).

[4] G. FIKSEL, S. C. PRAGER, W. SHEN, and M. R. STONEKING, Phys. Rev. Lett. **72** (1994) 1028.

[5] M. R. STONEKING, S. A. HOKIN, S. C. PRAGER, G. FIKSEL, H. JI, and D. J. DEN HARTOG, Phys. Rev. Lett. **73** (1994) 549.

[6] G. FIKSEL, A.F. ALMAGRI, D. CRAIG, M. IIDA, S.C. PRAGER, and J.S. SARFF, Plasma Sources Sci. Technol. **5** (1996) 78.

[7] Y.L. HO, Nucl. Fusion **31** (1991) 341.

[8] E. UCHIMOTO *et al.*, Phys. Plasmas **1** (1994) 3517.

[9] H. JI, S. C. PRAGER, A. F. ALMAGRI, J. S. SARFF, Y. YAGI, Y. HIRANO, K. HATTORI, AND H. TOYAMA, Phys. Plasmas **3** (1996) 1935.

[10] G. S. LEE, P. H. DIAMOND, and Z. G. AN, Phys. Fluids B **1** (1989) 99.

[11] A. R. JACOBSON and R. W. MOSES, Phys. Rev. A **29** (1984) 3335.

[12] D. J. DEN HARTOG and R. J. FONCK, Rev. Sci. Instrum. **65** (1994) 3238.

[13] S. HOKIN *et al.*, Phys. Fluids B **3** (1991) 2241.

[14] S. ORTOLANI and D. D. SCHNACK, *Magnetohydrodynamics of Plasma Relaxation*,World Scientific, Singapore (1993), 95-127.

[15] A. F. ALMAGRI *et al.*, Phys. Fluids B **4** (1992) 4080.

[16] D. J. DEN HARTOG *et al.*, Phys. Plasmas **2** (1995) 2281.

[17] M. YOKOYAMA, J. D. CALLEN, and C. C. HEGNA, "Evolution of Toroidal Flow Velocity During Locked Modes," to be published in Nuclear Fusion (1996).

[18] C. C. HEGNA, "Nonlinear Tearing Mode Interactions and Mode Locking in Reversed Field Pinches," to be published in Physics of Plasmas (1996).

[19] C.-S. CHIANG *et al.*, Bull. Am. Phys. Soc. **40** (1995) 1753.

[20] A. F. ALMAGRI *et al.*, Bull. Am. Phys. Soc. **40** (1995) 1753.

EXTERNAL DISTRIBUTION IN ADDITION TO UC-20

S.N. Rasband, Brigham Young University
R.A. Moyer, General Atomics
J.B. Taylor, Institute for Fusion Studies, The University of Texas at Austin
E. Uchimoto, University of Montana
F.W. Perkins, PPPL
O. Ishihara, Texas Technical University
M.A. Abdou, University of California, Los Angeles
R.W. Conn, University of California, Los Angeles
P.E. Vandenplas, Association Euratom-Etat Belge, Belgium
Centro Brasileiro de Pesquisas Firicas, Brazil
P. Sakanaka, Institute de Fisica-Unicamp, Brazil
Mme. Monique Bex, GANIL, France
J. Radet, CEN/CADARACHE, France
University of Ioannina, Greece
R. Andreani, Associazione EURATOM-ENEA sulla Fusione, Italy
Biblioteca, Istituto Gas Ionizzati, EURATON-ENEA-CNR Association, Italy
Plasma section, Energy Fundamentals Division Electrotechnical Laboratory, Japan
Y. Kondoh, Gunma University, Kiryu, Gunma, Japan
H. Toyama, University of Tokyo, Japan
Z. Yoshida. University of Tokyo, Japan
FOM-Instituut voor Plasmafysica "Rijnhuizen," The Netherlands
Z. Ning, Academia Sinica, Peoples Republic of China
P. Yang, Shandong University, Peoples Republic of China
S. Zhu, University of Science & Technology of China, People's Republic of China
I.N. Bogatu, Institute of Atomic Physics, Romania
M.J. Alport, University of Natal, Durban, South Africa
R. Storer, The Flinders University of South Australia, South Australia
B. Lehnert, Royal Institute of Technology, Sweden
Librarian, CRPP, Ecole Polytechnique Federale de Lausanne, Switzerland
B. Alper, Culham Laboratory, UK
A. Newton, UK

2 for Chicago Operations Office
5 for individuals in Washington Offices

INTERNAL DISTRIBUTION IN ADDITION TO UC-20
80 for local group and file